

PAPER • OPEN ACCESS

## Drought severity trend analysis based on the Landsat time-series dataset of 1998-2017 in the Iraqi Kurdistan Region

To cite this article: Ayad M. Fadhil Al-Quraishi *et al* 2021 *IOP Conf. Ser.: Earth Environ. Sci.* **779** 012083

View the [article online](#) for updates and enhancements.



**ECS** **240th ECS Meeting**  
Digital Meeting, Oct 10-14, 2021  
**We are going fully digital!**  
Attendees register for free!  
**REGISTER NOW**

# Drought severity trend analysis based on the Landsat time-series dataset of 1998-2017 in the Iraqi Kurdistan Region

Ayad M. Fadhil Al-Quraishi<sup>1\*</sup>, Heman Abdulkhaleq A. Gaznayee<sup>2</sup>, Joseph P. Messina<sup>3</sup>

<sup>1</sup>Surveying and Geomatics Engineering Department, Faculty of Engineering, Tishk International University, Erbil, 44001, Kurdistan Region, Iraq.

<sup>2</sup>Department of Forestry, College of Sciences of Agricultural Engineering, Salahaddin University, Erbil 44003, Kurdistan Region, Iraq.

<sup>3</sup>College of Arts and Sciences, University of Alabama, Tuscaloosa, AL, 35487, USA.

\* Corresponding author. Email: [ayad.alquraishi@tiu.edu.iq](mailto:ayad.alquraishi@tiu.edu.iq)

**Abstract.** Drought is a natural hazard that significantly impacts economic, agricultural, environmental, and social aspects and is characteristic of Iraq's climate, particularly the Iraqi Kurdistan Region (IKR). For studying the spatiotemporal characteristics of drought severity in the IKR, a time-series of 120 Landsat images (TM, 7 ETM+, and OLI sensors) over twenty years (1998-2017) was assembled. Twenty separate mosaics of six Landsat scenes were used to derive the Vegetation Condition Index (VCI). The VCI index was employed to capture the drought severity in the study area. Results revealed that 1999, 2000, and 2008 were the most severe drought years. The results also indicated that severe droughts increased by 29.1%, 25.0%, and 26.9 through 1999, 2000, and 2008, respectively. Furthermore, a drop in precipitation averages occurred in the two years and significantly reduced the VCI values. Statistical analysis exhibited significant correlations between the VCI and each precipitation, and crop yield was 0.81 and 0.478, respectively. It can be concluded that the IKR experienced severe to extremely severe agricultural droughts, which caused significant reductions in crop yields, particularly in 2000 and 2008.

**Keywords:** Drought severity, Landsat satellite image, VCI, Iraqi Kurdistan Region.

## 1. Introduction

Drought is a natural disaster that can occur in all regions with vastly different climates [1]. However, it is a common phenomenon in arid and semi-arid regions [2]. Drought can be simply defined as a deficit in precipitation, and terrestrial water storage, which adversely impacts agriculture and the environment [3]. It is often related to high temperatures and low moisture levels and is often associated with climate change [4]. The Intergovernmental Panel on Climate Change (IPCC, 2007, 2014) mentioned that global climate models offer two predictions linked to droughts: increases in temperature and precipitation decrease [5]. Although the common cause of drought is attributed to precipitation below normal levels, anthropogenic activities can also contribute to drought occurrences [6]. The sequence of drought development occurs when a drought event initially starts with a prolonged shortage in precipitation, meteorological drought and then develops into reduced soil available water and limited vegetation cover, known as an agricultural drought [7].

Drought and its effects on the Iraqi lands have been identified by the National Oceanic and Atmospheric Administration (NOAA) as "a lack in precipitation over an extended period, usually a season or more, resulting in water stress, causing adverse impacts on vegetation, animals, and/or people" [8]. Iraq's location in an arid and semi-arid area contributes to frequent droughts. Given increasing drought events numbers and severity, particularly during the last two decades, Iraq, among other countries, is where significant drought management actions must be developed and adopted [9]. At the same time, the annual perception averages have been declined in recent years [10]. The Iraqi



report 2009 considered the lack of rainfall at all rates to be the main reason for severe drought in the IKR [11]. The country has suffered several drought events from 2003 through 2017, which were resulted from different factors, such as low precipitations, higher temperatures, and a severe decline in its two main rivers discharges [12].

Furthermore, severe drought was recorded in the Iraqi Kurdistan Region (IKR) governorates, particularly in Erbil governorate in 1999, while Duhok governorate experienced moderate drought from 1986-1987, 1989-1991, 1999-2000, and 2007-2008. The IKR is the most vulnerable area to drought, as it is the country's main grain-growing area [11,13,14]. The meteorological data revealed that precipitation significantly decreased in 2008, and drought events severely hit the region [15]. From 1999 to 2002, Erbil governorate experienced low precipitation averages; thus, severe droughts events occurred in that harsh period. Moreover, it is experienced another drought period that started from 2007 to 2011, therefore, it might be considered as a vulnerable area to drought [16]. Similarly, Sulaimaniyah, the second governorate in the IKR, has also experienced severe droughts periods for nearly half a decade from 1994 to 1998. Additionally, similar observations were observed in the Duhok governorate in the same period [14].

Remote sensing (RS) techniques and indices, such as the Normalized Difference Vegetation Index (NDVI), can be used for monitoring effects of rainfall and drought, estimating net primary production of vegetation, crop growth, and crop yields as reported in several studies [17,18]. Time-series based spectral indices that adopt spatiotemporal drought analysis are broadly used to monitor climate change and human activities. Areas experiencing excessive rainfall low averages might cause damage to the vegetation cover. This could lead to a drought event, which misleads the detecting of drought if only the NDVI is used. Therefore, this can be avoided with a combination of temperature; since rainy weather usually occurs in temperatures favourable for vegetation [16]. The benefit of utilizing the VCI is to separate the fluctuations of NDVI resulting from short-term weather-related conditions and the fluctuations resulting from long-term ecosystem effects [17].

The VCI is more efficient than NDVI in capturing rainfall dynamics, especially in a uniform geographical area. It can also be employed to quantify the impact of weather on vegetation and its role in reflecting spatiotemporal vegetation variability [19, 20]. The vegetation condition index (VCI) derived from remote-sensing data has been widely used for drought monitoring [21]. However, the VCI, based on the NDVI, does not perform well in certain circumstances [22]. The utility of the VCI for monitoring drought conditions has been studied in various regions worldwide during critical periods of crop growth [23].

The study objectives were: 1) investigate spatiotemporal drought severity based on Landsat time-series VCI of 1998-2017; 2) state statistical relationships between VCI with each of rainfall averages, Digital Elevation Model (DEM), and latitude; 3) explore the historical frequency, duration, and spatial extent of drought episodes, supporting researchers, decision-makers, and environmental specialists in their decisions.

## **2. Materials and methods**

### *2.1 Study area*

The study area includes the entire territory of the IKR, situated in the northern part of Iraq (Fig. 1), between latitudes 34° 42' to 37° 22' N and longitudes 42° 25' to 46° 15' E, and bordering Syria in the west, Turkey in the north, and Iran in the east. The IKR covers 53,000 km<sup>2</sup> and includes three governorates; Erbil, Duhok, and Sulaimaniyah [24]. It is characterized by a semi-arid continental climate with a hot and dry summer and cold and wet winter [25]. Precipitation in the IKR exhibits high precipitation averages in its northern parts and low averages in the plains [26]. The annual rainfall averages vary between less than 100 mm in the southern parts up to 1,200 mm in the northeastern and mountainous parts. In general, rainfall usually occurs from October to May, while hotter summer months present little or no precipitation at all [27]. Based on precipitation averages, the IKR can be further classified into three different areas; 1) assured rainfall area (over 500 mm), 2) semi assured rainfall area (350-500 mm), and 3) unassured rainfall area (less than 350 mm) as shown in Fig. 1. The rained lands in the IKR represent 37.2% of the region's total agricultural lands [28,29].

### *2.2 Remotely sensed datasets*

For this study, 120 time-series scenes of Landsat 5 TM, Landsat 7 ETM+, and Landsat 8 OLI were assembled, distributed in six scenes for each year (Path/Rows:170/34, 170/35, 169/35, 169/34, 168/35, and 168/36) acquired from 1998 through 2017. Twenty mosaics, each including six scenes, were produced for each year of the study period from those images. Landsat datasets were downloaded from the United States Geological Survey (USGS). Images date clustered on April and May (according to its availability), given that most of the vegetation growth stages occur in April and May across the study area. ASTER GDEM V2 dataset with a spatial resolution of 30m, available from the NASA Reverb homepage, was downloaded and utilized as the DEM dataset (Fig. 2).

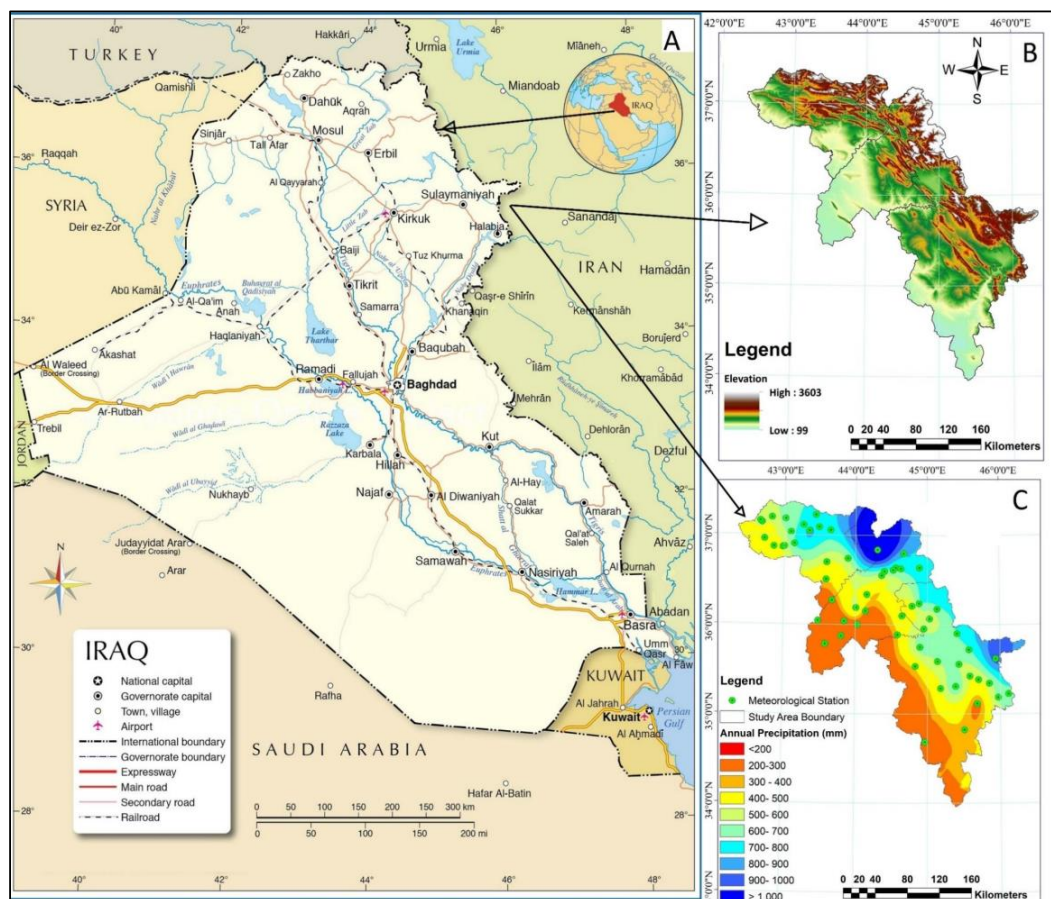


**Fig. 1** (A) Location map of the study area (B), Digital elevation model (DEM) of the IKR, and (C) Spatial distribution of the annual rainfall (mm/year) in the IKR during 1998 through 2017.

### 2.3 Preprocessing of satellite data

The Landsat images were delivered in a standardized, orthorectified format and geometrically corrected in datum WGS84 and projection UTM zone N38. All of the images were then converted from their original digital number (DN) values into the top of the atmosphere (ToA) reflectance values using ENVI ver. 5.3. Preprocessing for the images acquired by different Landsat satellites sensors was done to make them consistent with other sensors' images, which is an essential normalization process step in change detection research. The image registration process used the Landsat images of 1998 as bases with the corresponding features on each subsequent image registered to the respective base Landsat TM image of 1998. The RMS errors of the registration processes were less than 0.4 pixels. The registration processes have completed using ERDAS Imagine 2014.

### 2.4 Drought spectral index

The Vegetation Condition Index (VCI) was derived from the Landsat images of twenty using the following headings equations. The NDVI was utilized to produce the VCI images for twenty years.

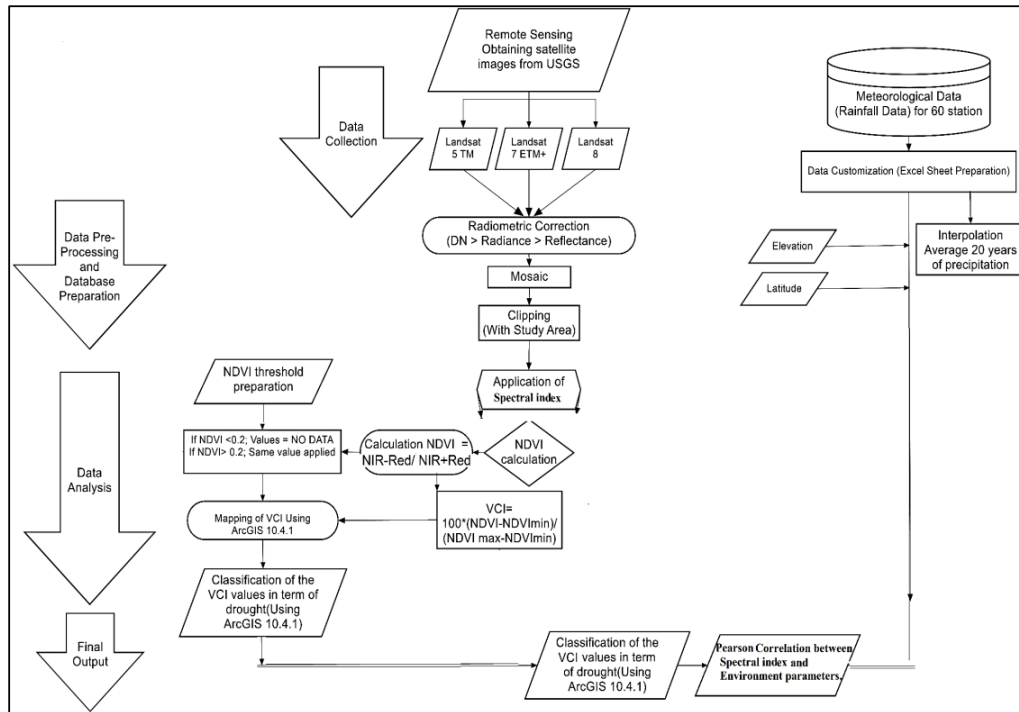


Fig. 2. Flowchart of the methodology adopted in the study.

2.4.1 Vegetation Condition Index (VCI)

The VCI was derived to differentiate the weather-related component of the NDVI from ecological factors [30]. It can be calculated using Eq. 1:

$$VCI = 100 * (NDVI - NDVI_{min}) / (NDVI_{max} - NDVI_{min}) \quad (1)$$

Kogan [30] proposed a Vegetation Condition Index (VCI) based on the relative Normalized Difference Vegetation Index (NDVI) change with respect to minimum historical NDVI value. The VCI, therefore, compares the current NDVI to the values observed in the same period in previous years within a specific pixel. Where NDVI represents an NDVI value of the current month,  $NDVI_{min}$  and  $NDVI_{max}$  denote the minimum and maximum of the NDVI values, respectively, throughout the observation. As a drought tool, VCI was employed by several studies, whereas the only VCI values were not enough precise descriptions of drought status [31]. VCI values were classified (Table 1) based on the classification developed by [32, 33].

Table 1. Classification of the VCI values in terms of drought according to Kogan (2002) [34].

Drought Category	Values
Extreme drought	$\leq 10$
Severe drought	$10 < \& \leq 20$
Moderate drought	$20 < \& \leq 30$
Mild drought	$30 < \& \leq 40$
No drought	$> 40$

### 2.5 Statistical analyses

Multivariable correlation analyses have been conducted to compute the relationships among the VCI and study variables (rainfall, elevation, and latitude) for the time series. The statistical analyses were completed using the SPSS ver. 25.

### 2.6 Reference data and ground truth

Reference data and ground truth consisted of classified land cover and soil attributes for the year 2017. Field trips conducted in 2017 in the IKR provided reference data for use to validate the VCI and TCI maps.

## 3. Results and discussion

### 3.1. Vegetation Cover based on (VCI)

VCI results reflected the severe drought events that prevailed in 1999, 2000, and 2008, VCI values ranged from 0 for non- showed that the most critical years for drought based on the VCI index were 1999, 2000, and 2008, whereas the vegetation cover was remarkably reduced compared with the other years through the investigation period. The drought peaked in 2000, its highest severity; thus, it is considered the driest year within the study period. Based on the spatial patterns of drought severity in the IKR, the results revealed that the entire study area experienced mild to severe drought from 1998 to 2017., particularly in 2000 and 2008. The year 2008 was a terrible drought year with severe conditions across the IKR, except for some small northern patches. The combined severe and very severe drought areas in the north, eastern, middle, and southern parts of the IKR were 8110.3 km<sup>2</sup> (39.4%), 5,544.6 km<sup>2</sup> (26.9%), 3,314.6 km<sup>2</sup> (16.1%), and 1,848.6 km<sup>2</sup> (9%), respectively. In general, the VCI (Table 2 and Figs 3-4) showed that the southern and middle parts of the IKR are the most affected areas by extreme droughts. Results also revealed that the IKR suffered a very severe drought in 2000 with 4,028.5 km<sup>2</sup> (60.5%), 1,596.2 km<sup>2</sup> (24.0%), 692.8 km<sup>2</sup> (10.5%), and 219.3 km<sup>2</sup> (0.6%) for Extreme Drought, Severe Drought, Moderate Drought, Mild Drought, and No Drought, respectively. On the other side, results of the second-highest area for Extreme Drought Classe (VCI≤10) revealed that the largest class area was recorded in 1999 with an expanded extreme drought area by 12,527.3 Km<sup>2</sup> (%44.7).

### 3.2 Pearson correlation analysis

The strength of statistical relationships among drought and the individual study variables using bivariate correlation analysis computed using SPSS ver. 25. The correlation matrix (Table. 3) allowed us to find the essential statistical relationships between each VCI and the study variables, such as rainfall, elevation, and latitude. Correlation coefficients of VCI with rainfall, elevation, and latitude for 1998 through 2017 were calculated and presented in Table 3. The results showed significant positive correlations between rainfall and VCI in all studied years (Table 3 and Fig.4). Results of correlation coefficients between precipitation, VCI, mean and area vegetation, crop area vegetation, and crop yield during the years from 1998 to 2017 (average of 20 years) calculated and presented (see Table 3).

The correlation between spectral index and precipitation was statistically significant, whereas drought indices showed significant differences at  $p < 0.01$  and  $p < 0.05$  confidence levels among the studied years. The results showed a significant positive relation ( $r = 0.535^*$  and  $0.478^*$ ) between the VCI and crop yield and crop area, respectively. The highest crop yield reduction occurred in 2000 and 2008 due to the agricultural drought influences (Table 4). Yield reductions can be attributed to the precipitation variability and needed to satisfy the minimum crop water requirements. Crop yield is generally correlated with VCI. Reduction of VCI and precipitation positively correlated with cereal crop yield revealed that the VCI index could monitor drought. A significant linear statistical correlation was found between the annual rainfall and VCI, which can be invested to predict and manage drought risk. The analysis for the 60 meteorological stations dataset showed better correlations between VCI and rainfall amounts. Study results (Fig.4) suggest that the frequency of various rainfall events and associated seasonal and annual rainfall over IKR is spatially heterogeneous as well as seasonal and

that the highest rainfall is found in the northeast and decreases toward the south. Through seasonal analysis, unsurprisingly, it was observed that there was a positive correlation between the crop production and rainfall of the region. This relationship demonstrates the dominance of rain-fed agriculture throughout the region.

**Table 2.** Areas and rate of the Drought Severity Categories based on VCI values in 1998 through 2017.

Year	Extreme Drought VCI≤10		Severe Drought 10<VCI≤20		Moderate Drought 20<VCI≤30		Mild Drought 30<VCI≤40		No Drought VCI> 40		Total Vegetation cover area	
	Area (km <sup>2</sup> )	Area (%)	Area (km <sup>2</sup> )	Area (%)	Area (km <sup>2</sup> )	Area (%)	Area (km <sup>2</sup> )	Area (%)	Area (km <sup>2</sup> )	Area (%)	(km <sup>2</sup> )	(%)
1998	9,686.2	36.6	6,474.1	24.5	4,761.4	18.0	3,051.2	11.5	2,501.0	9.4	26,474.0	100
1999	12,527.3	44.7	8,147.1	29.1	4,495.1	16.0	1,976.3	7.0	887.2	3.2	28,033.0	100
2000	4,028.5	60.5	1,596.2	25.0	692.8	10.5	219.3	3.4	25.6	0.6	6,562.4	100
2001	7,014.6	23.5	6,019.7	20.2	5,354.8	18.0	4,475.3	15.0	6,942.1	23.3	29,806.4	100
2002	8,013.6	26.6	6,734.4	22.3	5,505.4	18.3	4,150.0	13.8	5,759.2	19.1	30,162.5	100
2003	6,492.5	22.3	5,629.8	19.4	5,249.2	18.0	4,571.2	15.7	7,148.0	24.6	29,090.7	100
2004	7,069.1	23.3	6,483.5	21.4	5,897.3	19.5	4,864.0	16.1	5,965.3	19.7	30,279.1	100
2005	7,938.7	30.0	6,780.9	25.6	5,356.7	20.2	3,489.9	13.2	2,898.1	11.0	26,464.3	100
2006	7,807.0	27.4	5,584.1	19.6	4,903.2	17.2	4,214.7	14.8	6,002.2	21.1	28,511.1	100
2007	5,814.8	19.2	5,847.5	19.3	6,123.2	20.2	5,376.0	17.7	7,170.9	23.6	30,332.3	100
2008	8,110.3	39.4	5,544.6	26.9	3,314.6	16.1	1,848.6	9.0	1,791.8	8.7	20,609.8	100
2009	6,777.1	27.1	5,799.2	23.2	5,343.5	21.3	3,966.9	15.8	3,150.4	12.6	25,037.2	100
2010	7,237.9	25.0	6,026.7	20.9	5,252.3	18.2	4,336.3	15.0	6,041.6	20.9	28,894.7	100
2011	9,423.2	35.0	6,297.8	23.4	3,591.9	13.3	2,776.0	10.3	4,828.6	17.9	26,917.5	100
2012	5,409.5	20.5	5,365.7	20.3	5,202.7	19.7	4,445.2	16.8	5,978.3	22.6	26,401.4	100
2013	6,539.7	23.3	5,300.0	18.8	4,955.9	17.6	4,496.1	16.0	6,835.8	24.3	28,127.5	100
2014	7,105.1	23.0	6,442.7	20.9	5,882.1	19.0	4,784.9	15.5	6,669.8	21.6	30,884.7	100
2015	6,563.2	20.6	5,832.8	18.3	5,759.3	18.1	5,643.4	17.7	8,062.4	25.3	31,861.2	100
2016	7,807.9	24.2	7,397.0	22.9	6,995.1	21.6	5,493.9	17.0	4,621.2	14.3	32,315.1	100
2017	7,506.6	27.7	6,273.5	23.2	5,475.1	20.2	4,102.0	15.1	3,739.5	13.8	27,096.8	100

**Table 3.** Pearson Correlation between VCI index, crop area, crop yield, and annual average precipitation in the IKR.

	Crop area (Km <sup>2</sup> )	Crop yield (ton)	VCI	Precipitation (mm)
Crop area (Km <sup>2</sup> )	1	0.692**	0.535*	0.679**
Crop yield (ton)	0.692**	1	0.478*	0.533*
VCI	0.535*	0.478*	1	0.81**
Precipitation (mm)	0.679**	0.533*	0.81**	1

\*\* Correlation is significant at the 0.01 level (2-tailed).

\* Correlation is significant at the 0.05 level (2-tailed).

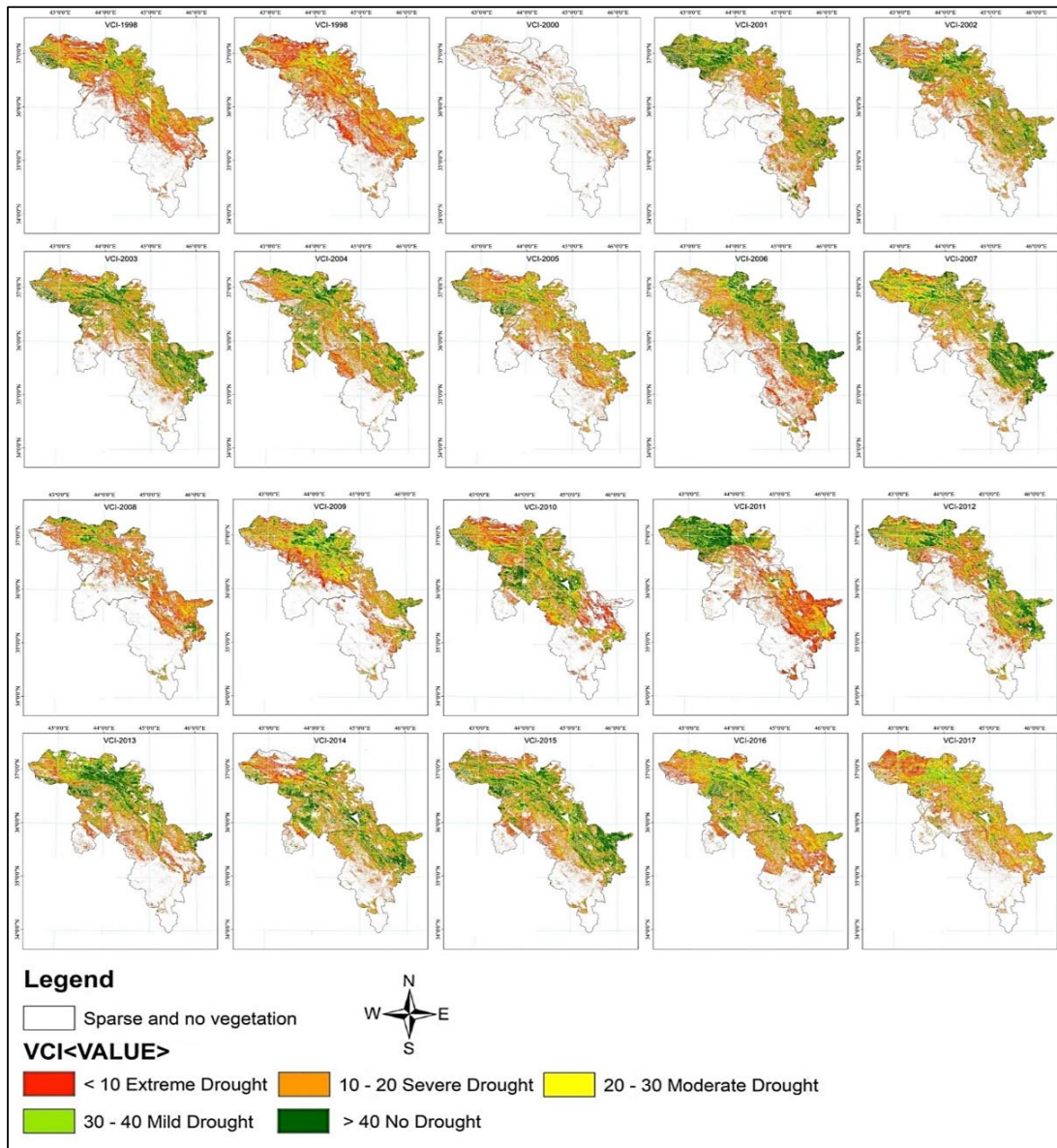


**Fig. 3.** Drought severity categories based on the VCI values in 1998 through 2017.

The present study attempts to identify the spatio-temporal agricultural drought over IKR using the Vegetation Condition Index (VCI) and comparing it with crop yield. Drought periods are identified where the twenty-year moving average is below the average of the reference period. The IKR results are presented separately and revealed that even if there are some differences in the trend across sites during the reference period, all locations experienced a reduction in precipitation and that severe drought affected the whole region, especially in the years 1998 1999 and 1999-2000. Almost all parts, from the north to the south, are considered drought-prone areas. All areas are considered highly vulnerable to it. For drought evaluation, the differences in water availability among governorates should be considered. Based on an analysis of the reference period's moving average, drought most evidently occurred in 1999 and 2000, 2008, and 2012. The sum of precipitation amounts measured for the twenty years has significantly decreased by nearly 40% compared to the same timescale period before 1999, 2000, 2008, and 2012. Thus, as observations, where the 20-years are moving average, show precipitation values upper the annual mean.

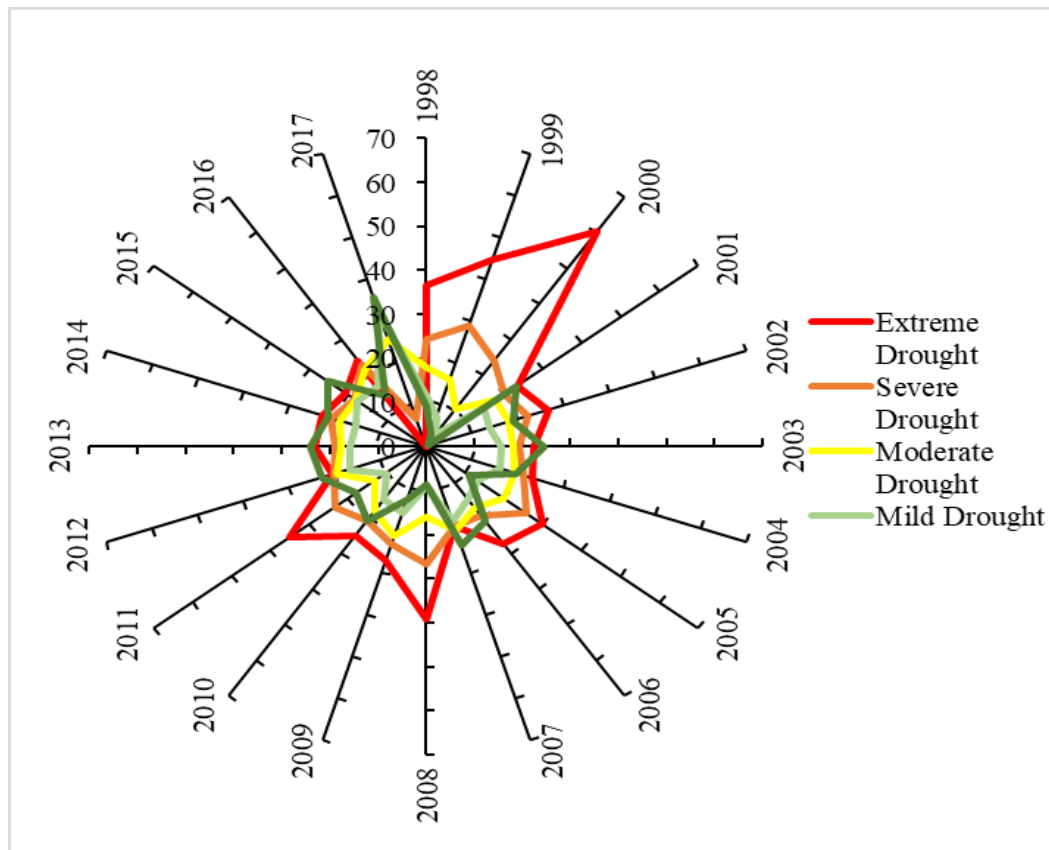


**Figure 4.** Temporal variation of percentage area of the VCI-based drought categories based on total vegetation cover each year.

#### 4. Discussion

Drought is defined as a lack of soil moisture. However, its impact on society is highly related to time, duration, frequency, magnitude, and place of occurrence [35]. Although there is a difference in intensity and extent of drought for each indicator, no doubt there is a difference in the ability and strength of each drought index to diagnose drought severity based on the vegetative cover areas. Ultimately, however, VCI results proved the severity of drought in 2000 and 2008. Maps of the VCI showed that most IKR areas experienced severe to very severe drought in the two years mentioned above (Fig.3 and 4). Consequently, the droughts can be attributed to the lack of precipitation and high land surface temperatures throughout the critical plant growth stage in 2000 and 2008. As mentioned in the previous sections, the northern and eastern parts of the IKR characterized by high altitude and have higher annual rainfall averages.

Time-series analysis for drought indices provides a framework for evaluating the drought situation in the area of interest.

Jackson et al. [36] reported that the VCI attempts to directly measure vegetation health, which could be affected by many factors, including water, insects, disease, nutrients. Vegetation stress that was detected other reasons than lack of water could cause the VCI to change [37]. Therefore, the indices can be employed as proxies for biomass production estimation, and the biomass reduction occurred when VCI dropped below 50 (the level indicating the beginning of vegetation stress). The VCI variations indicated that in April of the years 2000 and 2008, vegetation cover was stressed and that harmful drought conditions developed due to low rainfall averages and high temperatures. This decline was clearly shown in the VCI values. Therefore, the VCI can be effectively used for drought severity detection and mapping [38]. Precipitation is thus the key factor contributing to vegetation stress in these rain-fed agricultural areas. In this case, VCI had a higher correlation with precipitation and more than latitude. The southern part of the IKR shows a net decrease in vegetative cover during the time series. It may be affected by land-degradation processes, in part, caused by

droughts common in this area. At the same time, the forest lands in the northern part of IKR have deeper root systems than grasslands and croplands and are thus less sensitive to rainfall [39-41].

**Table 4.** Crop area and crop yield of Wheat and Barley from 1998 to 2017 (Ministry of Agriculture and Water Resources, 2017).

Years	Area/km <sup>2</sup>	Yields/ton
1997-1998	1,862.4	459,878.3
1998-1999	1,571.5	159,744.8
1999-2000	1,997.2	330,150.7
2000-2001	2,129.1	593,490.2
2001-2002	2,727.0	909,681.1
2002-2003	2,214.0	640,317.6
2003-2004	2,134.6	600,081.6
2004-2005	3,003.9	811,656.7
2005-2006	2,918.4	717,650.1
2006-2007	3,346.5	12,647.19
2007-2008	1,633.3	405,028.0
2008-2009	2,404.2	1,334.169
2009-2010	2,724.0	1,602.567
2010-2011	2,882.0	825,001.6
2011-2012	2,510.8	1,101.454
2012-2013	2,259.7	1,741.527
2013-2014	1,760.3	1,669.531
2014-2015	3,281.0	1,930.148
2015-2016	3,195.6	1,927.677
2016-2017	2,659.1	1,943.752

Many studies indicated that VCI presented a delayed response to the change of moisture conditions and that the previously accumulated soil water storage controls this reaction. According to [42], the VCI index based on NDVI is a better indicator of the moisture deficit than NDVI because it allows separating the short-term climate signal from the long-term ecological signal. The VCI enables comparison with simultaneously measured NDVI values under the different geographic conditions and different vegetation types. The highest yield reduction occurred in 2000 and 2008 due to agricultural drought events (Table 4). The reduction might be attributed to the precipitation amount's fluctuation to satisfy the minimum crop water requirement [27]. Crop yield is generally correlated with vegetation conditions; this result can be used to develop a relationship between precipitation with crop yield. Similar results were obtained by [43, 44], whereas the results of VCI were well explained by both meteorological data and impact data on crop yield. Therefore, VCI might be a more suitable index in identifying droughts in wheat and barley fields and other low water demand crops. VCI values indicate how much the vegetation has advanced or deteriorated in response to weather and how far vegetation development is from the potential maximum and minimum defined by the ecological limits [45, 46]. The results also revealed significant declines in the vegetative cover in the years 2000, 2008, and 2012, by 43.8%, 16.3%, and 10.9%, respectively [12,16]. Furthermore, a drop in precipitation averages has occurred in those three drought years and a significant reduction in the VCI values.

## 5. Conclusions

Landsat-based time series VCI have been used in this study for spatiotemporal drought characteristics in the IKR from 1998 to 2017. The results showed that in IKR, the vegetation health was severely affected by climatic factors, such as precipitation and temperature, particularly in 2000 and 2008. It was found that severe drought conditions prevailed during those two years over a large area of the IKR. The onset and extent of drought can be clearly observed when utilizing the VCI maps. Acute water stress is evident all over the study area during 1998, 2000, 2008, and 2012. Despite the prevalence of drought conditions over a large area during the years mentioned above, some areas in the IKR's eastern parts remained unaffected

by water stress and drought risk, and the northern parts are characterized by high altitudes and lands covered by forest trees and grasses. Furthermore, the northern parts of the IKR are characterized by a humid and sub-humid climate.

Spatial variation in vegetation health resulted from uneven distribution of rainfall, and geographical elevation significantly influences the variation of vegetation cover and land surface temperature in the study area. Since the northern parts of the IKR receive much higher rainfall averages than the western and the southern parts, even in drought years, it remains suitable for tree and shrub growth. However, even there, the vegetation condition was visibly stressed during the year 2000. The VCI showed good vegetation health over a large IKR area during 2002, 2005, 2011, and 2016. Some parts of the southwestern of the IKR were comparatively greener due to those years' sufficient rainfall.

Unlike the meteorological data available from sparsely distributed meteorological stations, Landsat time-series images based on the VCI index can successfully be employed for delineating the spatiotemporal drought severity characteristics in the IKR. The growing-season VCI appears to be more sensitive to long-term precipitation deficiencies. There was also significant spatial variability in the strength of the relationship between the VCI and the crop yield. The present study attempted to evaluate the spatiotemporal extent of agricultural drought over IKR using Landsat-based VCI, precipitation, and crop yield. It also proves the importance of remote sensing and GIS techniques for estimating drought-related stress in rain-fed crops.

**Acknowledgments:** The authors would like to thank the United States Geological Service (USGS) for free providing the Landsat datasets. We are also thankful to the Salahaddin University-Erbil, Kurdistan Region, Iraq, and the Ministry of Agriculture & Water Resources-Kurdistan Region Government (KRG), Iraq, for their valued support.

## References

- [1] Demisse G B, Tadesse T, Wall N, Haigh T, Bayissa Y and Shiferaw A 2019 Linking seasonal drought product information to decision makers in a data-sparse region: A case study in the Greater Horn of Africa *Remote Sens. Appl. Soc. Environ.* **14** 200–6
- [2] Jha S and Srivastava R 2018 Impact of drought on vegetation carbon storage in arid and semi-arid regions *Remote Sens. Appl. Soc. Environ.* **11** 22–9
- [3] Lloyd-Hughes B 2014 The impracticality of a universal drought definition *Theor. Appl. Climatol.* **117** 607–11
- [4] Trenberth K E 2011 Changes in precipitation with climate change *Clim. Res.* **47** 123–38
- [5] Van Loon A F, Gleeson T, Clark J, Van Dijk A I J M, Stahl K, Hannaford J, Di Baldassarre G, Teuling A J, Tallaksen L M, Uijlenhoet R, Hannah D M, Sheffield J, Svoboda M, Verbeiren B, Wagener T, Rangelcroft S, Wanders N, Van Lanen H A J 2016 Drought in the Anthropocene *Nat. Geosci.* **9** 89
- [6] Tigkas D, Vangelis H and Tsakiris G 2018 Drought characterisation based on an agriculture-oriented standardised precipitation index *Theor. Appl. Climatol.* 1–13
- [7] Al-Quraishi A M F and Negm A M 2019 *Environmental Remote Sensing and GIS in Iraq*, Springer Water, Springer, Cham. ISBN 978-3-030-21344-2
- [8] Aghakouchak A, Farahmand A, Melton F S, Teixeira J, Anderson M C, Wardlow B D and Hain C R 2015 Reviews of geophysics remote sensing of drought: Progress, challenges *Rev. Geophys.* **53** 1–29
- [9] Hamad R, Balzter H and Kolo K 2017 Multi-Criteria Assessment of Land Cover Dynamic Changes in Halgurd Sakran National Park (HSNP), Kurdistan Region of Iraq, Using Remote Sensing and GIS *Land* **6** 18
- [10] Fadhil A M 2013 Sand dunes monitoring using remote sensing and GIS techniques for some sites in Iraq *PIAGENG 2013 Intell. Information, Control. Commun. Technol. Agric. Eng.* **8762** 876206
- [11] Mustafa Y T 2020 Spatiotemporal Analysis of Vegetation Cover in Kurdistan Region-Iraq using MODIS Image Data **01** 1–6
- [12] Al-Quraishi A M F, Gaznayee H A A, Crespi M 2020 Drought Trend Analysis in Sulaimaniyah (Iraqi Kurdistan Region) for the Period 1998-2017 using Remote Sensing and GIS. *J. of Arid Land* (In Press).
- [13] Tinti A 2017 Water Resources Management in the Kurdistan Region of Iraq A *POLICY Rep. Am. Univ. Iraq, Sulaimani (AUIS)*. 20
- [14] UNESCO 2014 Integrated drought risk management– DRM executive *Natl. Framew. IRAQ AN Anal. Rep. MARcH Second ed.*
- [15] Fadhil A M 2011 Drought mapping using Geoinformation technology for some sites in the Iraqi Kurdistan region *Int. J. Digit. Earth* **4** 239–57. doi:https://doi.org/10.1080/17538947.2010.489971
- [16] Gaznayee H A A; Al-Quraishi A M F 2019 Analysis of Agricultural Drought, Precipitation, and Crop

- Yield Relationships in Erbil Province, the Kurdistan region of Iraq based on Landsat time-series msavi2 J. Adv. Res. Dyn. Control Syst. **11** 536–45. doi: <https://doi.org/10.5373/JARDCS/V11SP12/20193249>
- [17] Kogan F N 1995 Application of vegetation index and brightness temperature for drought detection *Adv. Sp. Res.* **15** 91–100
- [18] Zhang L, Yao Y, Bei X, Jia K, Zhang X and Xie X 2019 Assessing the Remotely Sensed Evaporative Drought Index for Drought Monitoring over Northeast China
- [19] Kogan F N 2002 Droughts of the Late 1980s in the United States as Derived from NOAA Polar-Orbiting Satellite Data *Bull. Am. Meteorol. Soc.* **76** 655–68
- [20] Unganai L S and Kogan F N 1998 Drought monitoring and corn yield estimation in southern Africa from AVHRR data *Remote Sens. Environ.* **63** 219–32
- [21] Singh R P, Roy S and Kogan F 2003 Vegetation and temperature condition indices from NOAA AVHRR data for drought monitoring over India *Int. J. Remote Sens.* **24** 4393–402
- [22] Vilanova R S, Delgado R C, da Silva Abel E L, Teodoro P E, Silva Junior C A, Wanderley H S and Capristo-Silva G F 2020 Past and future assessment of vegetation activity for the state of Amazonas-Brazil *Remote Sens. Appl. Soc. Environ.* **17** 100278
- [23] Kogan F N 1997 Global drought watch from space *Bull. Am. Meteorol. Soc.* **78** 621
- [24] Mustafa Y T 2015 Mapping and Estimating Vegetation Coverage in Iraqi Kurdistan Region using Remote Sensing and GIS *Gen. Dir. Hortic. For. Rangeland, Minist. Agric. Water Resour. Kurdistan Reg. Iraq-FINAL Rep. 2015 FINAL REPO* 1–136
- [25] Saeed M A 2012 Analysis of Climate and Drought Conditions in the Fedral *Journal, Int. Sci. Sci. Environ.* 953
- [26] UNDP 2012 Capacity Assessment for Drought Risk Management in Iraq *Interdiscip. Res. Consult. Amman 11942, Jordan. United Nations Dev. Program. Final Repo*
- [27] Gaznayee H A A; and Al-Quraishi A M F 2019 Analysis of Agricultural Drought's Severity and Impacts in Erbil Province, the Iraqi Kurdistan Region based on Time-Series NDVI and TCI Indices for 1998 through 2017 *Jour Adv Res. Dyn. Control Syst.* **11** 287–97. doi: <https://doi.org/10.5373/JARDCS/V11I11/20193198>.
- [28] Eklund L, Persson A and Pilešjö P 2016 Cropland changes in times of conflict, reconstruction, and economic development in Iraqi Kurdistan *Ambio* **45** 78–88
- [29] Karim T H, Keya D R and Amin Z A 2018 Temporal and spatial variations in annual rainfall distribution in Erbil province *Outlook Agric.* **47** 59–67
- [30] Kogan F N 1986 Climate constraints and trends in global grain production *Agric. For. Meteorol.* **37** 89–107
- [31] Sahoo R N, Dutta D, Khanna M, Kumar N and Bandyopadhyay S K 2015 Drought assessment in the Dhar and Mewat Districts of India using meteorological, hydrological and remote-sensing derived indices *Nat. Hazards* **77** 733–51
- [32] Du L, Tian Q, Yu T, Meng Q, Jancso T, Udvardy P and Huang Y 2013 A comprehensive drought monitoring method integrating MODIS and TRMM data *Int. J. Appl. Earth Obs. Geoinf.* **23** 245–53
- [33] Kogan F N 1990 Remote sensing of weather impacts on vegetation in non-homogeneous areas *Int. J. Remote Sens.* **11** 1405–19
- [34] Rimkus E, Stonevicius E, Kilpys J, MacLulyte V and Valiukas D 2017 Drought identification in the eastern Baltic region using NDVI *Earth Syst. Dyn.* **8** 627–37
- [35] Manatsa D, Mukwada G, Siziba E and Chinyanganya T 2010 Analysis of multidimensional aspects of agricultural droughts in Zimbabwe using the Standardized Precipitation Index (SPI) *Theor. Appl. Climatol.* **102** 287–305
- [36] Jackson R B, Canadell J, Ehleringer J R, Mooney H A, Sala O E and Schulze E D 1996 A global analysis of root distributions for terrestrial biomes *Oecologia* **108** 389–411
- [37] Kogan F, Stark R, Gitelson A, Jargalsaikhan L, Dugrajav C and Tsooj S 2004 Derivation of pasture biomass in Mongolia from AVHRR-based vegetation health indices *Int. J. Remote Sens.* **25** 2889–96
- [38] Quiring S M and Ganesh S 2010 Evaluating the utility of the Vegetation Condition Index (VCI) for monitoring meteorological drought in Texas *Agric. For. Meteorol.* **150** 330–9
- [39] Karnieli A, Bayasgalan M, Bayarjargal Y, Agam N, Khudulmur S and Tucker C J 2006 Comments on the use of the Vegetation Health Index over Mongolia *Int. J. Remote Sens.* **27** 2017–24
- [40] Mahyou H, Karrou M, Mimouni J, Mrabet R and Mourid M El 2010 Drought risk assessment in pasture arid Morocco through remote sensing *African J. Environ. Sci. Technol.* **4** 845–52
- [41] Vogt J, Viau A, Beaudin I, Niemeyer S and Somma F 1998 Drought monitoring from space using empirical indices and physical indicators *Proc. Int. Symp. 'Satellite-Based Obs. A Tool Study Mediterr. Basin' 23 – 27 Novemb. 1998, Tunis, Tunis.* 9

- [42] Jain, S K, Keshri R, Goswami A 2010 Application of meteorological and vegetation indices for evaluation of drought impact: 325 a case study for Rajasthan, India, *Nat. Hazards*, **54**, 643–656, doi:10.1007/s11069-009-9493-x, 2010.
- [43] Seiler R A, Kogan F and Sullivan J 1998 AVHRR-based vegetation and temperature condition indices for drought detection in Argentina *Adv. Sp. Res.* **21** 481–4
- [44] Rojas O, Vrieling A and Rembold F 2011 Assessing drought probability for agricultural areas in Africa with coarse resolution remote sensing imagery *Remote Sens. Environ.* **115** 343–52
- [45] Gebrehiwot T, van der Veen A and Maathuis B 2011 Spatial and temporal assessment of drought in the Northern highlands of Ethiopia *Int. J. Appl. Earth Obs. Geoinf.* **13** 309–21
- [46] Gaznayee, H A A, Al-Quraishi A M F, Al-Sulttani A H A 2020 Drought Spatiotemporal Characteristics based on the Vegetation Condition Index (VCI) in Erbil, the Iraqi Kurdistan Region from 1998 to 2017 *The 2<sup>nd</sup> International Conference of Al-Karkh University of Science (ISC2/KUS2020)*